Ecological functions and environmental fate of exopolymers of Acidobacteria

Costa, O.Y.A.

Chapter 5

Identification of bacterial and fungal co-occurrence networks during assimilation of acidobacterial extracellular polymers in soil

Ohana Y. A. Costa, Agata Pijl, Eiko E. Kuramae

Submitted for publication

Abstract

Acidobacteria are one of the most abundant and ubiquitous bacterial phyla in soil but little information is available on their physiology and interactions with the other members of the soil microbial community. *Acidobacteria* produce copious amounts of extracellular polymeric substances (EPS) with unique sugar composition that could be used as a nutrient source by other microorganisms. Here, we investigated the impact of the amendment of EPS of *Granulicella* sp. strain WH15 (WH15EPS) to soil on assembly and interactions of the active bacterial and fungal communities. The addition of purified WH15EPS to the topsoil litter increased microbial activity compared with the unamended control, as measured by CO_2 respiration. Stable isotope probing (SIP) over a period of 35 days revealed that WH15EPS was assimilated by *Planctomycetes*, *Verrucomicrobia, Ascomycota* and *Basidiomycota.* Several taxa incorporated WH15EPS, including *Singulisphaera*, which was the most abundant genus in the labeled treatment. Co-inertia analysis suggested overall relationships between *Bacteria* and *Fungi*. Fungal groups were mainly connected positively to each other and negatively connected to bacterial groups, indicating competition for the carbon sources derived from the EPS. In addition, *Singulisphaera* had mostly positive connections, suggesting a potential cooperation in EPS metabolization. Our study revealed the potential interactions and structures of the co-occurrence network of active microorganisms able to metabolize WH15EPS differed from those of the control treatments, demonstrating that the analysis of co-ocurrence networks based only on total DNA may not reflect real co-occurrence among microorganisms. Furthermore, potential interactions that were not observed before, such as the connections between *Singulisphaera* and groups of *Planctomycetes* or *Acidobacteria,* can be unraveled by more specific and targeted metabolism studies.

Keywords: *Acidobacteria*, EPS, Stable Isotope Probing, *Planctomycetes*, Co-occurrence; Carbohydrates

1. Introduction

Acidobacteria are abundant bacterial phyla in soil, constituting 20–50% of the soil bacterial community (Kuramae *et al.*, 2012, Navarrete *et al.*, 2013, Pan *et al.*, 2014, Kielak *et al.*, 2016, Kielak *et al.*, 2016). However, little information is available on the physiology, ecological function, and impact of *Acidobacteria* on the soil environment (Kielak *et al.*, 2016) because their slow growth under standard laboratory conditions has resulted in a relatively small number of cultured representatives. Consequently, the factor(s) responsible for the prevalence and successful adaptation of *Acidobacteria* and their relationships with other soil-inhabiting microbes remain unknown (Kielak *et al.*, 2016).

Acidobacteria such as strains Ellin6076 and Ellin345 (Ward *et al.*, 2009), *Terriglobus tenax* (Whang *et al.*, 2014) and *Granulicella* sp. strains WH15 and 5B5 (Kielak *et al.*, 2017) produce extracellular polymeric substances (EPS). EPS are biopolymers secreted by a variety of microorganisms and mainly comprise carbohydrates, proteins and DNA. The role of EPS depends on the ecological niche and natural dwelling environment of the microorganism (Costa *et al.*, 2018). EPS production has been implicated in the long-term survival of *Acidobacteria* in several environments due to its protective properties (Kielak *et al.*, 2017). EPS also may serve as nutrient sources for other microorganisms (Flemming & Wingender, 2010), however the use of EPS from *Acidobacteria* as a nutrient has never been investigated in cross-feeding experiments.

The assimilation of EPS as a carbon source by active microorganisms can be investigated with stable isotope probing (SIP). SIP is a powerful technique that evaluates the incorporation of compounds labelled with heavy isotopes, such as ^{13}C, ^{18}O and ^{15}N, into the cell components of microorganisms metabolizing a specific substrate. Thus, SIP reflects the active microorganisms involved in the metabolism of a specific compound. SIP has been used to investigate the microorganisms responsible for the degradation of different compounds in many environments (Madsen, 2006), including labelled glucose (Verastegui *et al.*, 2014), methanol (Ginige *et al.*, 2004), phenol (Padmanabhan *et al.*, 2003), salicylate and anthracene (Singleton *et al.*, 2005). The use of SIP to investigate EPS has been limited to a single study identifying microorganisms that assimilate the EPS of *Beijerinckia indica* (Wang *et al.*, 2015). In this context, in the present study, EPS from *Granulicella* sp. strain WH15 was applied as a carbon source to soil sampled from the site where this strain was isolated, and the active bacterial and fungal community assemblages and interactions in the soil during a 35-day period were evaluated by SIP.

2. Material and Methods

2.1. Soil Sampling

Four topsoil-litter mixed samples were collected in the spring of 2017 from the Wolfheze forest in the Netherlands (Table 1). Samples were taken from topsoil (0 to 5 cm) adjacent to fallen tree trunks. The collected samples were pooled, sieved (4 mm mesh) and immediately used for SIP incubation with EPS from *Granulicella* sp. strain WH15 (WH15EPS). The physicochemical properties of the topsoil-litter samples were determined (Eurofins Agro BV, Wageningen, NL) and are presented in Table 2.

Table 1: Coordinates of the sampling sites.

Site number	Latitude	Longitude
1	51°59'14.5"N	5°47'32.7"E
2	51°59'15.9"N	5°47'29.5"E
3	51°59'15.7"N	5°47'27.7"E
4	51°59'14.8"N	5°47'23.2"E

Table 2: Physicochemical properties of topsoil-litter samples.

Component	Unit	Average (Sd)	Component	Unit	Average (Sd)
total N	mg N/kg	16535±3217	**CEC**	%	81±0.0
C/N ratio		20±6	**CEC**	mmol+/kg	214±42
Available N	kg N/ha	252±187	**B**	µg B/kg	488±4.2
pH		3.05±0.1	**Cu**	µg Cu/kg	48±9.9
OM	%	55.8±3.5	**Fe**	µg Fe/kg	3070±466.7
Na	mg Na/kg	34.5±4.9	**Mn**	µg Mn/kg	101920±9362.1
P	mg P/kg	42.65±6.4	**Zn**	µg Zn/kg	8860±693.0
K	mg K/k	218±11.3	**Clay**	%	5.5±0.7
Ca	kg Ca/ha	13±0	**Silt**	%	10±14.1
Mg	mg Mg/kg	175±7.1	**Sand**	%	27.5±12.0

Sd: standard deviation

2.2. [^{13}C]-Labeled and Unlabeled EPS Production

Granulicella sp. strain WH15 was grown on PSY5 solid medium (Campanharo *et al.*, 2016) containing 3% (wt/vol) fully ^{13}C-labeled glucose as the sole carbon source or unlabeled glucose for unlabeled control EPS production. The plates were incubated at 30 °C for 3 days and then at 20 °C for 27 days. The polysaccharide portion of EPS was extracted and purified according to the method described by Liu and Fang (2002), with modifications. EPS and cells of strain WH15 (~5 ml) were scraped from the plates into 50-ml Falcon tubes, and the volume was adjusted to 10 ml with sterile water. Sixty microliters of 36.5% formaldehyde was added to each sample and incubated at 4 °C for 1 h. Next, 4 ml of 1 M NaOH was added and incubated at 4 °C for 3 h. The cells were then pelleted by centrifugation at 9,000 xg for 40 min. The supernatants were filtered (0.2 µm membranes, Millipore) at room temperature, and monosaccharides were removed by dialysis in SnakeSkin™ Dialysis Tubing (3500 Da) (Thermo Fisher Scientific, Massachusetts, USA) against demineralized water at 4 °C for 48 h. The solutions were frozen at -80 °C for 12 h and then freeze-dried at -80 °C for 72 h.

Before freeze-drying, the DNA concentration in the EPS solution was determined in a Qubit fluorometer using a broad-range Quant-iT™ dsDNA Assay Kit (Invitrogen, Carlsbad, California, USA). EPS protein concentrations were determined by a Pierce™ Modified Lowry Protein Assay Kit (Thermo Fisher Scientific, Massachusetts, USA). The total carbohydrate content was estimated by the phenol-sulfuric acid method (DuBois *et al.*, 1956) modified for 96-well plates (Masuko *et al.*, 2005) with glucose as the standard. After purification, the EPS contained ~400 mg/ml carbohydrates, ~1% protein and undetectable amounts of DNA. The monosaccharide composition of WH15EPS was previously characterized (Kielak *et al.*, 2017) and comprises xylose (41.8%), mannose (10.25%), glucose (13.55%), galactose (26.12%), rhamnose (0.065%), glucuronic acid (8.09) and galacturonic acid (0.085%).

2.3. Stable Isotope Probing (SIP) Incubation

One milliliter of Milli-Q sterile water was added to the freeze-dried EPS immediately before inoculation in soil to facilitate a homogeneous distribution within the soil. Five grams (wet weight) of soil with 0.05% (wt/wt) WH15EPS (labeled and unlabeled controls) or without EPS was added to a 120-ml bottle, which was sealed with a butyl rubber stopper and incubated at room temperature (22 °C) in the dark. Each treatment (labeled EPS, unlabeled EPS and control without EPS) had six replicates. All vials were uncapped and aired every 4 days to maintain oxic conditions and prevent $^{13}CO_2$ cross-feeding. The vial headspace CO_2 was monitored daily via gas chromatography (GC) (Trace GC Ultra, Thermo Fisher Scientific, Massachusetts, USA). For incubations with [^{13}C]-labeled EPS, the headspace CO_2 $^{13}C/^{12}C$ ratio was monitored via GC combustion isotope ratio mass spectrometry (GC/C/IRMS) (GC IsoLink II™ IRMS System, Thermo Fisher Scientific, Massachusetts, USA). For DNA extraction, 0.5 g were sampled from the vials on days 8, 24 and 35, which corresponded to 10, 25 and 43% $^{13}CO_2$ headspace enrichment, respectively. The differences in CO_2 emissions on the different days were analyzed by analysis of variance (ANOVA one-way repeated measurements) using mixed-effects models ('lmerTest' (Kuznetsova *et al.*, 2017) and 'psycho' (Makowski, 2018) packages in R).

2.4. DNA Extraction and Fractionation

DNA was extracted from 250 mg of soil with or without ^{13}C-labeled/unlabeled substrates with the PowerSoil® DNA Isolation Kit (MO BIO Laboratories, Inc) according to the manufacturer's instructions. DNA was quantified by a spectrophotometer (NanoDrop™ 2000, Thermo Fisher Scientific, Massachusetts, USA) and visualized by 1.0% agarose gel electrophoresis and ethidium bromide staining. For gradient fractionation, 2 µg of DNA was combined with CsCl (1.72 g/ml) and gradient buffer (100 mM Tris-HCl pH 8.0, 100 mM KCl, 1mM EDTA) in an ultracentrifugation tube (PA UltraCrimp 1.8 ml, ThermoFisher Scientific, Massachusetts, USA) (Neufeld *et al.*, 2007) and ultracentrifuged at 125,395 xg (Discovery 120SE ultracentrifuge, ThermoFisher Scientific, Massachusetts, USA) under vacuum at 20 °C for 65 h. Gradient

fractionation resulted in 18 DNA fractions of approximately 100 µl each. The density of each fraction was measured with a refractometer (AR200, Reichert Technologies, New York, USA) to confirm gradient formation. DNA was precipitated from the CsCl with polyethylene glycol solution (30% PEG6000, 1.6 M NaCl) and glycogen (20 µg/µl), washed with 70% ethanol, and eluted in 30 µl of 10 mM Tris-HCl buffer, pH 8.0. The DNA concentration of each fraction was determined in a Qubit 4 Fluorometer (ThermoFisher Scientific, Massachusetts, USA) using a Quant-iT™ dsDNA HS Assay Kit (Invitrogen, Carlsbad, California, USA). The unlabeled substrate incubations were used as controls to determine the expected position of labeled soil DNA in the CsCl density gradients.

2.5. PCR, Sequencing and Sequence Processing of 16S rRNA Gene and ITS Data

Amplicon library preparation and high-throughput sequencing were performed using the "heavy" DNA fractions pooled within each sample replicate as well as the total DNA of both the amended and unamended controls. The V3-V4 region of the 16S rRNA gene and the internal transcribed spacer 2 (ITS1) region were targeted for bacteria and fungi, respectively. For bacteria, the V3-V4 region of 16S rRNA gene was targeted by using 515F (5'-GTGCCAGCMGCCGCGGTAA-3') as forward primer and 806R (5'-GGACTACHVGGGTWTCTAAT-3') (Bergmann *et al.*, 2011) as reverse primer. For fungi, the Internal Transcribed Spacer 1 (ITS1) region was targeted by using primers ITS1F (5′-CTTGGTCATTTAGAGGAAGTAA-3′) and ITS2 (5′-GCTGCGTTCTTCATCGATGC-3′) (White *et al.*, 1990). The amplification steps and Illumina MiSeq PE250 sequencing were performed at McGill University and Génome Québec Innovation Centre (Montréal, Québec, Canada). The sequences were deposited in the European Nucleotide Archive (ENA; https://www.ebi.ac.uk/ena) under the accession number PRJEB29719.

2.6. Processing and statistical analyses of 16S rRNA gene and ITS data

Raw sequencing data were processed through Hydra pipeline version 1.3.3 (Hollander, 2017) implemented in Snakemake (Koster & Rahmann, 2012). Reads were first quality filtered, by trimming adapters sequences and removing PhiX contaminants, using BBDuk2 from the BBMap tool suite (Bushnell, 2015). Paired-ends were merged using the fastq_mergepairs option from vsearch (Rognes *et al.*, 2015). The ITS1 region was extracted from ITS sequence dataset using ITSx version 1.011 (Bengtsson-Palme *et al.*, 2013). Next, vsearch was employed to cluster all reads into OTUs through the UPARSE strategy by dereplication, sorting by abundance with at least two sequences and clustering using the UCLUST smallmem algorithm (Edgar, 2010). Chimeriq sequences were detected and removed using the UCHIME algorithm in de-novo mode (Edgar *et al.*, 2011) implemented in VSEARCH. Before dereplication step, all reads were mapped to OTUs with the usearch_global method implemented in VSEARCH to generate an OTU table and converted to BIOM-Format (McDonald *et al.*, 2012). For 16S rRNA sequences, the taxonomic information for each OTU was then added to the BIOM file by aligning the sequences to the SILVA database (release 128) (McDonald *et al.*, 2012) using SINA

classifier (Pruesse *et al.*, 2012). For ITS sequences, the taxonomic information was added to the BIOM file by running the RDP Classifier re-trained on the UNITE database release 7.2 (Kõljalg *et al.*, 2013). Fungal OTUs were assigned to functional guilds using the annotation tool FUNGuild (Nguyen *et al.*, 2016).

2.7. Multivariate Analyses of 16S rRNA Gene and ITS Data

Statistical analyses were performed in RStudio version 1.1.423 running R version 3.4.4 (R Core Team, 2015). OTUs with less than 2 counts across all samples and chloroplast and mitochondrial sequences were discarded. Prior to alpha and beta diversity analyses, the data were rarefied to the size of the smallest sample (4,243 reads for the 16S rRNA gene and 7,797 for ITS region data). The 'Phyloseq' package (McMurdie & Holmes, 2013) was used to calculate the number of observed OTUs, Shannon and Inverse Simpson diversity indices, and Chao1 and ACE diversity estimators. Significant differences in the estimators between treatments were evaluated through parametric and non-parametric tests, including ANOVA, Kruskal-Wallis and Tukey's HSD tests (package 'agricolae' (Mendiburu, 2017)). Bray-Curtis distance matrices constructed using the rarefied datasets were used for principal coordinate analysis (PCoA) using the *capscale* function from the 'vegan' package (v. 2.4.6 (Oksanen *et al.*, 2018)). Group dissimilarities were tested by permutational multivariate analysis of variance (PERMANOVA) using the function *Adonis* from the 'vegan' package. To compare the structures of the bacterial and fungal communities within treatments, co-inertia (COIA) analysis of the Hellinger transformed datasets (Legendre & Gallagher, 2001) was performed using the function *coinertia* of the package 'ade4' (Dray & Dufour, 2007) as described by Schlemper et al. (Schlemper *et al.*, 2017) . Potential interactions between bacterial and fungal genera within treatments were investigated via SparCC correlation coefficients, with default parameters and 100 bootstraps (Friedman & Alm, 2012). Networks were built with significant interactions ($p<0.05$) at $|r| > 0.75$, and co-occurrence was visualized by Cytoscape (Shannon, 2003) and Gephi version 0.9.2 (https://gephi.org/). Topological parameters (numbers of nodes and edges and node degree number) were calculated using the network analyzer tool (Doncheva *et al.*, 2012) pre-installed in Cytoscape. Other plots were generated using 'ggplot2' (Wickham, 2016) and the *plot* function in R.

3. Results

3.1. CO_2 Measurements

The CO_2 emissions of the microcosms were 7,500 ppm CO_2/day initially and progressively decreased during incubation. Average CO_2 emissions were 1.3 times higher in the EPS-amended samples than in the unamended controls. At the end of the incubation, the EPS-amended microcosms produced 1.9 times more CO_2 than the unamended controls.

Headspace $^{13}CO_2$ enrichment increased throughout the incubation period, reaching 43% of the headspace in the labeled samples at day 35 (Figure 1). The differences in CO_2 emissions between treatments and p-values are shown in Table 3.

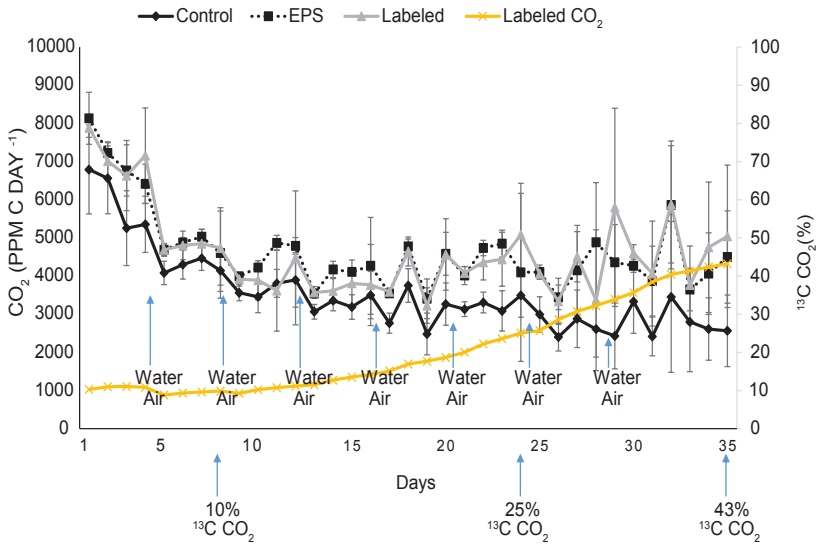

Figure 1: CO_2 emission. CO_2 production during total incubation period. Control: control without EPS; EPS: control containing ^{12}C-EPS; Labeled: incubation with ^{13}C-EPS; Labeled CO_2 percentage: $^{13}CO_2$ emitted during ^{13}C-EPS sample incubation; water: days when samples were hydrated; air: days when samples were aired.

5

Table 3: Contrast between CO_2 emission curves and statistical p-values.

Contrast	Difference	p-value
Unlabeled EPS -Control	1094.94	0.012356
Labeled EPS-Control	1058.11	0.01646
Unlabeled EPS – Labeled EPS	-36.83	0.994963

3.2. Gradient Fractionation

The density profiles of the DNA extracted from soils incubated with ^{13}C-EPS exhibited small changes compared with those of the control DNA from the ^{12}C-EPS incubations (Figure S1). “Heavy” fractions were chosen at densities at which little total DNA was detected in the control sample fractions (Figure S1). Among the 6 replicates, two from day 8 (L2D8 and L6D8) had “heavy” DNA in higher-density fractions, probably due to variations in the CsCl density centrifugation.

3.3. Sequencing and Alpha Diversity

High-throughput sequencing generated 1,250,548 and 828,045 good-quality sequences for

the bacterial 16S rRNA gene and fungal ITS region, respectively. Good's coverage (Table 4) indicated that the number of sequences reads covered 96.2%-98.4% of the bacterial diversity and 99.1-99.9% of the fungal diversity in the samples. Overall, for the 16S rRNA samples, the "heavy" fraction samples at all time points had significantly lower richness and diversity values than the unamended and ^{12}C-EPS-amended controls. Moreover, the ^{12}C-EPS-amended samples had lower richness and diversity values than the unamended samples (Figure S2). Similar to the 16S rRNA gene samples, the richness and diversity values of the ITS region were lower in the "heavy" fraction samples compared with the controls. This tendency was most obvious at days 24 and 35, whereas at day 8, the richness of the "heavy" fraction was not significantly different from that of the controls (Figure S3).

Table 4: Good's coverage for 16S rRNA gene and ITS region sequences within treatments.

16S rRNA gene sequences			**ITS region sequences**		
Treatment	**Day**	**Good`s coverage**	**Treatment**	**Day**	**Good`s coverage**
Control	8	96.2	Control	8	99.3
Unlabeled EPS	8	96.4	Unlabeled EPS	8	99.2
"Heavy" fraction	8	97.4	"Heavy" fraction	8	99.6
Control	24	96.3	Control	24	99.2
Unlabeled EPS	24	96.9	Unlabeled EPS	24	99.3
"Heavy" fraction	24	98.4	"Heavy" fraction	24	99.9
Control	35	96.3	Control	35	99.0
Unlabeled EPS	35	97.0	Unlabeled EPS	35	99.4
"Heavy" fraction	35	98.3	"Heavy" fraction	35	99.8

3.4. Community Structures

PERMANOVA (p=1.00e-04) showed that the bacterial communities differed significantly between the different treatments, days and treatment:day interactions, with the "heavy" fractions on days 24 and 35 clustering separately from the controls and the day 8 "heavy" fraction in the PCoA plot (Figure 2a). The bacterial communities clearly clustered according to treatments and days, with the first two axes of the PCoA explaining 70.5% of the variation. The fungal community patterns at different time points were less clear than those of the bacterial community. The fungal communities were more spread throughout the PCoA plot (Figure 2b). However, the heavy fractions on days 24 and 35 also clustered separately from the control samples and the day 8 "heavy" fraction. PERMANOVA (p value = 9.999^{e-05}) indicated significant differences between treatments, days and treatment:day interactions, with the first two axes of the PCoA explaining 27.8% of the variation among samples.

Co-inertia analysis revealed significant co-structures between the bacterial and fungal communities for all treatments (p<0.5). The first 2 co-inertia axes explained 80.4% ("heavy" fraction), 61.8% (EPS amended control) and 59.9% (unamended control) (cumulative projected inertia) of the total variance in the bacterial-fungal assessments (Figure 2cde). In addition, the bacterial and fungal groups at the genus level that contributed most to the co-

variance between samples were identified, which reflected the differences in abundances among time points (Figure S4).

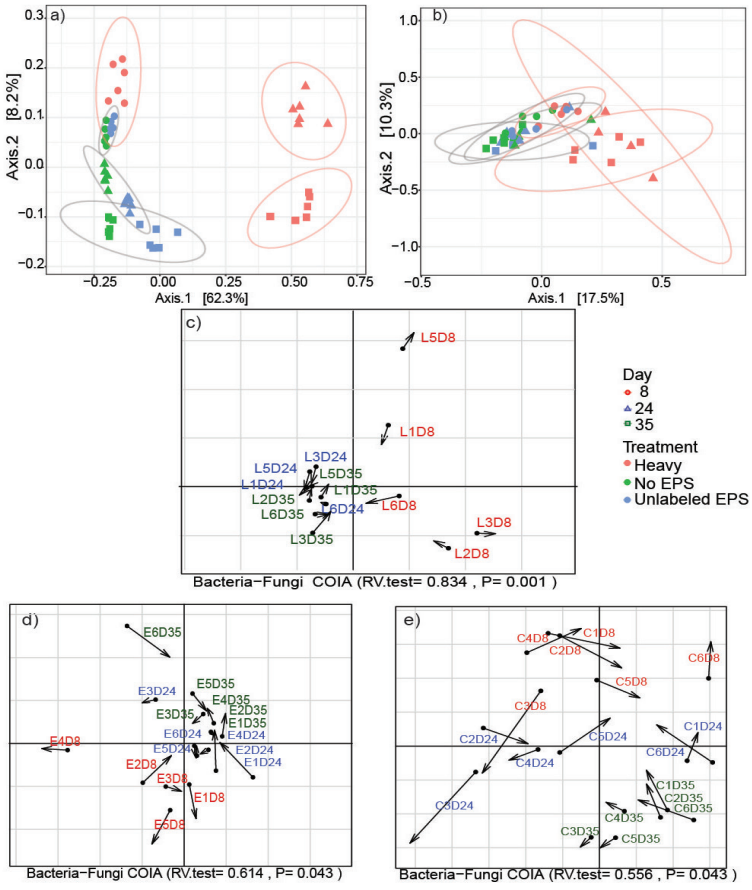

Figure 2: Co-inertia (COIA) and Principal Coordinate Analysis (PCoA) of microbial communities based on Bray-Curtis distances **a)** Bacterial community PCoA clustering of normalized and Hellinger-transformed rRNA gene 16S data **b)** Fungal community PCoA clustering of normalized and Hellinger-transformed ITS 1 region data. Co-inertia (COIA) analysis between PCoAs of **a)** bacterial and **b)** fungal community composition of samples amended with **c)** ^{13}C EPS, **d)** ^{12}C EPS and **e)** unamended samples. Samples from day 8 are colored in red, samples from day 24 are colored in blue and samples from day 35 are colored in in green.

3.5. Bacterial Community Beta Diversity

Twenty-two groups at the phylum level were observed in all samples. At day 8, the most abundant phylum in all samples was *Proteobacteria* (32.01%-39.7%) (Figure S5a). At day 24, the separation between microbial communities observed in the PCoA analysis became evident. The most abundant phylum was *Planctomycetes* in the "heavy" fraction (59.79%) but *Proteobacteria* in both control treatments (28.56%-31.23%) (Figure S5a). At day 35, *Planctomycetes* (60.79%) was still the most abundant phylum in the "heavy" fraction samples (Figure S5a), and *Proteobacteria* (25.65%-25.74%) remained the most abundant phylum in

the controls.

At the genus level, 220 groups were found in all samples. At day 8, unclassified *Pedosphaeraceae* was the most abundant group in the "heavy" fraction and the unamended control (12.34% and 13.04%, respectively). In the ^{12}C-EPS-amended treatment, the most abundant genus was *Rhodanobacter* (12.12%) (Figure 3a).

At day 24, Singulisphaera was the most abundant genus in the "heavy" fraction samples (27.79%) but represented only approximately 1.07-1.28% of the sequences in the control treatments. In both control treatments, unclassified Pedosphaeraceae (10.91%-14.36%) was the predominant group (Figure 3a).

At day 35, uncultured *Pirellulaceae* (36.21%) was the most abundant group in the "heavy"

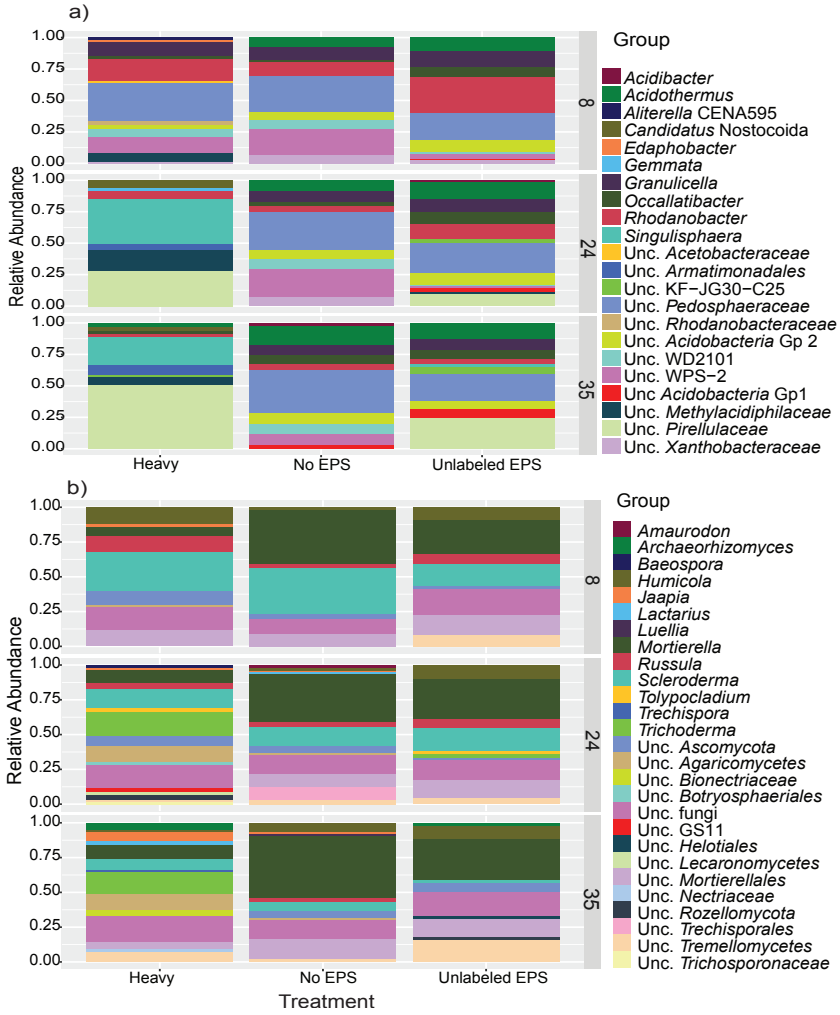

Figure 3: Relative abundance of microbial genera. Relative abundance of **a)** bacterial and **b)** fungal groups at genus level in 'heavy' fraction, EPS amended (Unlabeled EPS) and unamended (No EPS) controls at all time points (days 8, 24, 35). Only genera with >3% abundance are shown.

fraction, followed by *Singulisphaera* (16.22%). In the unamended control, the most abundant group was unclassified *Pedosphaeraceae* (16.52%), while in the amended control, the predominant group was uncultured *Pirellulaceae* (12.14%) (Figure 3a).

3.6. Fungal Community Beta Diversity

At the phylum level, 11 groups were observed in all samples. At days 8 and 24, *Basidiomycota* was the most abundant phylum in all samples (35.92%-43.16%) (Figure S5b). At day 35, the predominant group was *Basidiomycota* in the "heavy" fraction samples (38.7%) but *Mortierellomycota* in the unamended control (33.36%). In the ^{12}C-EPS amended control samples, *Ascomycota* (33.87%) was the most abundant phylum (Figure S5b).

At the genus level, 282 groups were observed in all samples. At day 8, the most abundant genus was *Scleroderma* in the "heavy" fractions (18.02%) but *Mortierella* in both control treatments (22.39%) (Figure 3b). At day 24, *Trichoderma* (15.67%) was the most abundant genus in the "heavy" fraction samples. In both control treatments, *Mortierella* was the most abundant genus (15.31%-21%) (Figure 3b). At day 35, unclassified fungi in the "heavy" fraction samples increased and were the most abundant group (15.21%), followed by *Trichoderma* (12.69%). *Mortierella* remained the most abundant genus in both control treatments (15.63%-24.96%) (Figure 3b). Analysis with FUNGuild assigned guilds to approximately 60% of the OTUs. The guild assignments demonstrated that all treatments, regardless of time point, were dominated by ectomycorrhizal fungi, soil saprotrophs and undefined saprotrophs (Figure S6).

3.7. Co-occurrence Network Analyses

3.7.1. Heavy fraction

The co-occurrence network of "heavy" fraction samples (Figure 4a) incorporated 59 nodes and 377 edges, with 51 bacterial nodes and 8 fungal nodes. At the genus level, 2 bacterial groups had connections with fungi, and 2 fungal groups were connected to bacteria. In total, 139 of the 377 connections were negative. The network contained several densely connected nodes, with 15 nodes having more than 20 neighbors each. The group with the highest number of connections was a *Planctomycetes* group, unclassified *Gemmataceae* (31 neighbors). Other groups with high connectivity were uncultured *Solirubrobacteraceae* (30 neighbors), unclassified *Armatimonadales* and *Acidothermus* (29 neighbors each). We also analyzed the bacterial genus identified as the most abundant in the "heavy" fractions, *Singulisphaera*, as well as the WH15EPS producer genus, *Granulicella*. In this treatment, *Singulisphaera* and *Granulicella* had 23 and 21 neighbors, respectively. Both genera had mainly positive connections (20 for *Singulisphaera* and 12 for *Granulicella*). No fungal group was connected to *Singulisphaera,* which was mainly connected to *Planctomycetes* and *Actinobacteria* (Figure 4d). The groups associated with *Singulisphaera* and *Granulicella* are described in Table S1. No strong associations were detected between *Granulicella* and

Singulisphaera. The most abundant fungal genus, *Trichoderma*, did not have any strong correlation.

3.7.2. ^{12}C-EPS-amended control

The network for the ^{12}C-EPS-amended control (Figure 4b) contained 29 nodes and 46 edges, with 18 bacterial nodes and 11 fungal nodes. Two bacterial groups interacted with fungi, and 3 fungal groups interacted with bacteria. No group had more than 10 neighbors, the

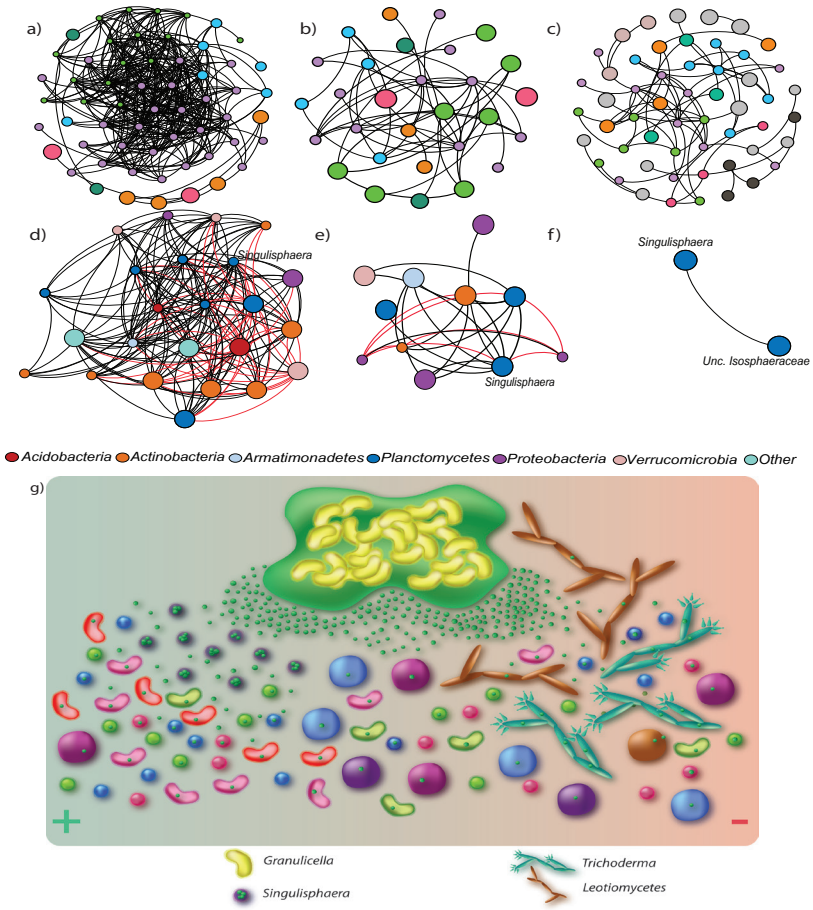

Figure 4: Co-occurrence networks and conceptual framework of the interactions of microorganism during WH15EPS assimilation. Total networks for **a)** "heavy" fraction; **b)** Unlabeled EPS control; **c)** NO EPS control (colors represent modularity classes); First neighbors of *Singulisphaera* genus in each treatment: **d)** "heavy" fraction; **e)** Unlabeled EPS control; **f)** NO EPS control (network nodes are genera). The size of the nodes represents the number of neighbors. Black edges represent positive correlations; red edges represent negative correlations. The size of each node is proportional to the number of connections (degree); **g)** Cartoon illustrating simplified hypothetical relationships among microorganisms during the metabolization of the EPS produced by *Granulicella* sp. strain WH15. *Singulisphaera* genus possessed negative (right (-)) correlations, as well as positive correlations (left (+)) with other bacterial genera. Negative associations suggest competition for the substrate, while positive associations suggest mutualism, via exchange of nutrients.

maximum number of neighbors of a node in this network. *Singulisphaera* and uncultured *Pirellulaceae* had the highest number of neighbors (10), followed by *Rhodanobacter*, Unclassified KF-JG30-C25 and uncultured *Solirubrobacteraceae*, with 6 neighbors each. In this treatment, *Granulicella* did not have any strong connections. *Singulisphaera* had only 2 negative connections, with *Dyella* and *Rhodanobacter* (Figure 4e). The associations of *Singulisphaera* are described in Table S2.

3.7.3. Unamended control

The network for the unamended control (Figure 4c) possessed 54 nodes and 66 edges, with 41 bacterial and 13 fungal nodes. Among all associations, 2 bacterial groups interacted with fungi, and 3 fungal groups interacted with bacteria. No groups had more than 10 neighbors. Genus *Burkholderia-Caballeronia-Paraburkholderia* had the highest amount of neighbours (10), followed by *Conexibacter* (7 neighbours), *Dyella* and uncultured *Acidobacteriaceae* subgroup 1 (6 neighbors each). *Singulisphaera* had only one positive connection to unclassified *Isosphaeraceae* (Figure 4f). *Granulicella* did not have any strong association.

4. Discussion

Here, we investigated the assimilation of EPS produced by *Granulicella* sp. strain WH15, a member of *Acidobacteria*. The ^{13}C-labeled biopolymer was applied to topsoil-litter samples, and high-throughput sequencing of the bacterial 16S rRNA gene and fungal ITS1 region identified the main EPS metabolizers. To increase the probability of finding true interactions, the mixed topsoil-litter was collected from the same forest site where *Granulicella* sp. strain WH15 was isolated (Valášková *et al.*, 2009).

Although the degradation of bacterial-produced biopolymers has been explored previously (cellulose produced by the bacterium *Gluconacetobacter xylinus* (Verastegui *et al.*, 2014, Wang *et al.*, 2015), indican from *Beijerinckia indica* (Wang *et al.*, 2015), and fructan from *Lactobacillus reuteri* (van Bueren *et al.*, 2015)), the metabolism of EPS produced by *Acidobacteria* and its ecological implications have not been investigated. The addition of purified WH15EPS to the topsoil-litter increased microbial activity compared with the unamended control, as measured by CO_2 respiration. The incorporation of the labeled EPS was confirmed by the increase in $^{13}CO_2$ release during incubation, which ranged from 10% to 43% of total headspace CO_2. The amount of $^{13}CO_2$ emitted varies according to the complexity of the substrate used for incubation and the capacity of the microbial community to degrade it (2012). Although the labeled material was clearly incorporated, the amount of “heavy” DNA recovered was lower than that reported in other SIP studies (Zhang *et al.*, 2016), likely due to the complexity of the substrate, a heteropolysaccharide composed of 7 different monosaccharides (Kielak *et al.*, 2017), and competition with the carbon present in the litter material (approximately 50% of

organic matter). Longer incubation times can improve the recovery of "heavy" DNA; however, a limitation of this strategy is that it also increases the possibility of cross-feeder enrichment (Verastegui *et al.*, 2014).

Alpha and beta diversity

The alpha diversity indices of the bacterial communities in the "heavy" fractions indicated lower richness and diversity than the amended and unamended controls at all sampling points, reflecting the selection of microorganisms capable of metabolizing the added EPS, particularly at day 35. These dynamics, however, were not as consistent for the fungal communities.

At day 8, the genus *Rhodanobacter* predominated in the EPS-amended control; however, the group unclassified *Pedosphaeraceae* was the most abundant in the "heavy" fraction and in the unamended control. *Rhodanobacter* is a genus of the family *Xanthomonadaceae* (*Proteobacteria*) found in soils featuring decomposition of aromatic compounds (Nalin *et al.*, 1999, Uhlik *et al.*, 2012, Song *et al.*, 2016) and forest litter (Štursová *et al.*, 2012, Verastegui *et al.*, 2014). *Pedosphaeraceae* (subdivision 3) is an uncharacterized family within the phylum *Verrucomicrobia*, which, like *Acidobacteria,* is widespread among terrestrial environments and has few cultivated representatives (Spring *et al.*, 2016).

Among the fungal communities, the genus *Scleroderma* was the most abundant in the "heavy" fractions and the second most dominant in the control samples after the genus *Mortierella* (which was also present in the heavy fraction). *Scleroderma* is a common, widespread ectomycorrhizal genus that produces macroscopic sporocarps in leaf litter, grass, bare soil or soil adjacent to forests (Jeffries, 1999). *Mortierella* is a root-colonizing endophytic fungus. Members of this globally distributed genus live as saprobes in soil on decaying organic material and dominate fungal communities in natural ecosystems (Johnson *et al.*, 2018).

The significant differences in the bacterial and fungal communities among all treatments were most evident at the later time points, and therefore enrichment of any specific microbial genus in the "heavy" fraction could not be observed at day 8. Several genera and phyla appeared to incorporate WH15EPS, possibly due to the ready hydrolysis of the biopolymer by exoenzymes already present in the litter material at the time of incubation.

At day 24, in the bacterial communities, clear enrichment of the phylum *Planctomycetes* could be observed in the "heavy" fraction samples, reaching approximately 60% of the total sequence number, with the genus *Singulisphaera* as the most abundant. At day 35, the enrichment of *Planctomycetes* persisted, with the genus *Singulisphaera* among the predominant genera but overcome by another group of *Planctomycetes*, uncultured *Pirellulaceae.* At the genus level, the total abundance of *Planctomycetes* was distributed among *Singulisphaera*, *Candidatus Nostocoida* and unclassified groups such as uncultured *Pirellulaceae* and "WD2101 soil group". *Planctomycetes* inhabit a variety of environments, including aquatic and terrestrial habitats as well as extremely acidic environments (Schlesner, 1994, Wang *et*

al., 2002, Ivanova & Dedysh, 2012, Faria *et al.*, 2018). *Planctomycetes* are highly abundant and phylogenetically diverse, especially in *Sphagnum*-dominated wetlands, where they can account for up to 54% of the total amount of 16S rRNA gene sequences (Moore *et al.*, 2015). Members of this phylum have unusual features, such as invaginations of the cytoplasmic membrane (Wiegand *et al.*, 2018). Although the functions of *Planctomycetes* are not clearly understood, they possess a wide range of hydrolytic capabilities, which would explain the promotion of their enrichment by the metabolization of the complex heteropolysaccharide WH15EPS. Using a transcriptome approach, Ivanova *et al*. (2017) observed that cellulose, xylan, pectin and chitin induced responses by different groups of *Planctomycetes*. The genus *Singulisphaera* responded significantly to pectin and xylan amendment. Members of the order *Phycisphaerales* and genus *Zavarzinella* also responded to xylan, while group WD2101 were responsive to cellulose and chitin. Another study by Ivanova *et al*. (2017) further supported the high glycolytic potential of *Planctomycetes.* In that study, a comparative genomic analysis of 4 members of the family *Isosphaeraceae*, namely *Isosphaera pallida*, *Singulisphaera acidiphila*, *Paludisphaera borealis* and the uncharacterized strain SH-PL62S, identified several CAZYmes from major families (GH5, GH13, GH57) as well as potential α-mannosidase, α-rhamnosidase and glucuronyl hydrolase activities. In addition, several CAZYmes not affiliated with currently recognized enzymes were found, demonstrating that these bacteria have the ability to use a wide range of natural carbohydrates and undiscovered glycolytic potential. Furthermore, *Singulisphaera acidiphila* is capable of hydrolyzing several polysaccharides, such as laminarin, pectin, chondroitin sulfate, aesculin, pullulan, lichenan, xylan and gelatin (Kulichevskaya *et al.*, 2008). Similar to the current study, Wang *et al*. (2015) reported enrichment of *Planctomycetes* by indican EPS of *Beijerinckia indica*. Indican is a biopolymer composed of glucuronic acid, glucose and glycerol-manno-heptose, indicating that *Planctomycetes* can decompose complex biopolymers.

Another group found in higher proportions in the "heavy" fractions at days 24 and 35 was uncultured *Methylacidiphilaceae.* This group belongs to the phylum *Verrucomicrobia*, which has few cultivated representatives but has been revealed to have hydrolytic capabilities in cultivation-independent studies. Martinez-Garcia *et al*. (2012) demonstrated that members of *Verrucomicrobia* have high hydrolytic potential and encode a wide spectrum of glycoside hydrolases, carbohydrate lyases and esterases in their genomes, indicating that they are well-equipped with enzymes for carbohydrate metabolism. Cardman *et al*. (2014) demonstrated that fluorescently labeled laminarin and xylan preferentially associated with *Verrucomicrobia* and proposed that this phylum is involved in polysaccharide hydrolysis.

Within the fungal communities, at day 24, an increase in the proportions of the genus *Trichoderma* and groups of unclassified fungi was observed in the "heavy" fraction compared with both the amended and unamended controls. *Trichoderma* is a genus of filamentous ascomycete fungi present in soils or growing on wood, bark and other fungi (mycoparasite) (Druzhinina *et al.*, 2011). This genus is highly opportunistic and adaptable to

several environments, with some strains applied for biocontrol of fungal phytopathogens. *Trichoderma reesei* is capable of decomposing woody and herbaceous materials and is an important industrial producer of hemicellulolytic enzymes (Martinez *et al.*, 2008, Druzhinina *et al.*, 2011).

As expected, the classification of fungal sequences in guilds in the current study revealed that the most abundant fungi were ectomycorrhizal (ECM) fungi and saprotrophs related to organic material decomposition (Valášková *et al.*, 2009, Urbanová *et al.*, 2015). Many species of ECM fungi act as decomposers based on the expression of extracellular enzymes (Bödeker *et al.*, 2009). Burke et al. (2014) indicated that enzyme activity varies greatly among ECM fungi, with some species producing enzymes at levels equivalent to those of saprotrophic fungi.

Co-occurrence and active interactions

Co-inertia analysis revealed significant co-variance between the fungal and bacterial communities, suggesting overall relationships between kingdoms. However, the co-occurrence networks showed that the overall number of connections between microbes was higher in the "heavy" fraction (377) than in either control treatment. The number of fungal genera connected to bacterial genera was lowest in the "heavy" fraction co-occurrence network (2), indicating that potential direct interactions between kingdoms did not increase during the assimilation of the EPS. Shorter arrows in co-inertia analysis for the heavy fraction, however, indicated a stronger relationship between bacterial and fungal communities, which could be due to indirect exchange of metabolites and use of fungal byproducts. Nonetheless, the assimilation of the EPS induced an increase in the potential interactions particularly among bacterial taxa, as observed in the number of edges in the "heavy" fraction network (377). These dynamics were not observed in the EPS-amended control network; nevertheless, not all taxa in this treatment are directly involved in the metabolism of the biopolymer. In addition, *Singulisphaera* had fewer potential interactions, with a variety of microorganisms from different phyla that have either cellulolytic capacity or the ability to remove toxic compounds (Valášková *et al.*, 2009, Kielak *et al.*, 2016). *Granulicella* did not show any strong connection with any taxa in both control treatments.

Fungi are thought to be the main players in the decomposition of recalcitrant materials such as lignocellulose, followed by bacterial decomposition of polysaccharides and polymeric compounds (Boer *et al.*, 2005, Romaní *et al.*, 2006). In the "heavy" fraction, however, only 8 fungal groups, such as Unclassified *Leotiomycetes* and the white-rot genus *Hypholoma* were observed. The fungal groups were mainly positively connected to each other, and negatively with unclassified groups of *Planctomycetes*, indicating competition for the carbon resources derived from the EPS, which hypothesis is supported by the high glycolytic capacity observed in both groups of microorganisms.

The most abundant bacterial genus in the "heavy" fraction, *Singulisphaera*, had mostly positive connections, especially with other groups of *Planctomycetes*, *Actinobacteria* and

Verrucomicrobia, suggesting potential cooperation for metabolizing WH15EPS. Several studies demonstrate that those groups of bacteria have glycolytic and detoxifying capacities, producing several enzymes that could be involved in the degradation of the EPS and resource sharing (Martinez-Garcia *et al.*, 2012, Uhlik *et al.*, 2012, Ivanova *et al.*, 2017). In addition, no direct correlation was found between *Singulisphaera* and the EPS producer *Granulicella,* which suggests that the metabolism of WH15EPS by *Singulisphaera* and enrichment of the genus did not negatively impact the abundance of *Granulicella*. This might be because of high amount of EPS added in the microcosm experiment. By contrast, *Granulicella* had a negative correlation with groups of *Actinobacteria,* demonstrating a potential competition, where *Actinobacteria* are metabolizing WH15EPS and impacting negatively *Granulicella*. *Actinobacteria* are widely spread in the environment and play an essential role in carbon cycling, presenting a wide range of extracellular enzymes (Lacombe-Harvey *et al.*, 2018). Furthermore, the presence of *Granulicella* in the heavy fraction demonstrates the capacity of the genus to use EPS as a carbon source; however, there is no experimental evidence that the producer strain is able to metabolize its own EPS.

It must be noted that the analysis of co-occurrence networks derived from labeled and unlabeled treatments demonstrated that the treatment based on unlabeled total DNA may not reflect real co-occurrence among microorganisms, suggesting this that type of analysis can yield misleading ecological inferences.

Several bacterial and fungal taxa have the ability and potential to metabolize the EPS of *Granulicella* sp. strain WH15. It is not possible to quantify the amount of EPS produced only by this genus in the natural environment; however, our study revealed active interactions between microorganisms in their natural habitat when EPS as added as carbon source. In addition, the structure of the co-occurrence network of microorganisms able to metabolize EPS differed from those in the control treatments, particularly in unlabeled EPS control demonstrating that hidden potential interactions can be unraveled by more specific metabolism studies. Finally, the number of potential associations with uncultured and unclassified taxa reinforces that further efforts are needed to characterize these groups to better understand their functions in the environment.

Acknowledgments

We would like to thank Wietse de Boer for helping with the sampling local, Hans Zweers for the GC measurements, Késia Lourenço for helping with soil analyses and Jos Raaijmakers and Marcio Leite for comments on the manuscript. O.Y.A. Costa was supported by an SWB grant from CNPq [202496/2015-5] (Conselho Nacional de Desenvolvimento Científico e Tecnológico).

Supplementary Material

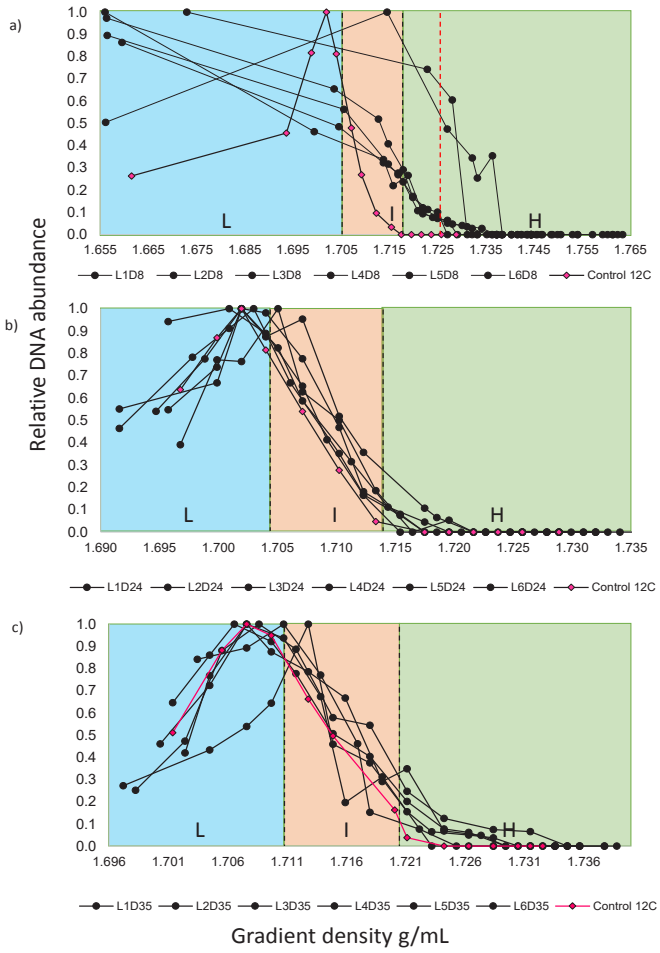

Figure S1: Gradient fractionation. Relative DNA concentrations in CsCl gradient fractions from total DNA extracted at **a)** day 8; **b)** day 24; **c)** day 35. The Y axis indicates the relative DNA concentration recovered from each fraction, with the highest concentration set equal to 1. L (blue) = Light fraction, I (orange) = intermediate fraction, H (green) = heavy fraction. The red dotted line in figure a) indicates the start of the heavy fraction for replicates L2D8 and L6D8.

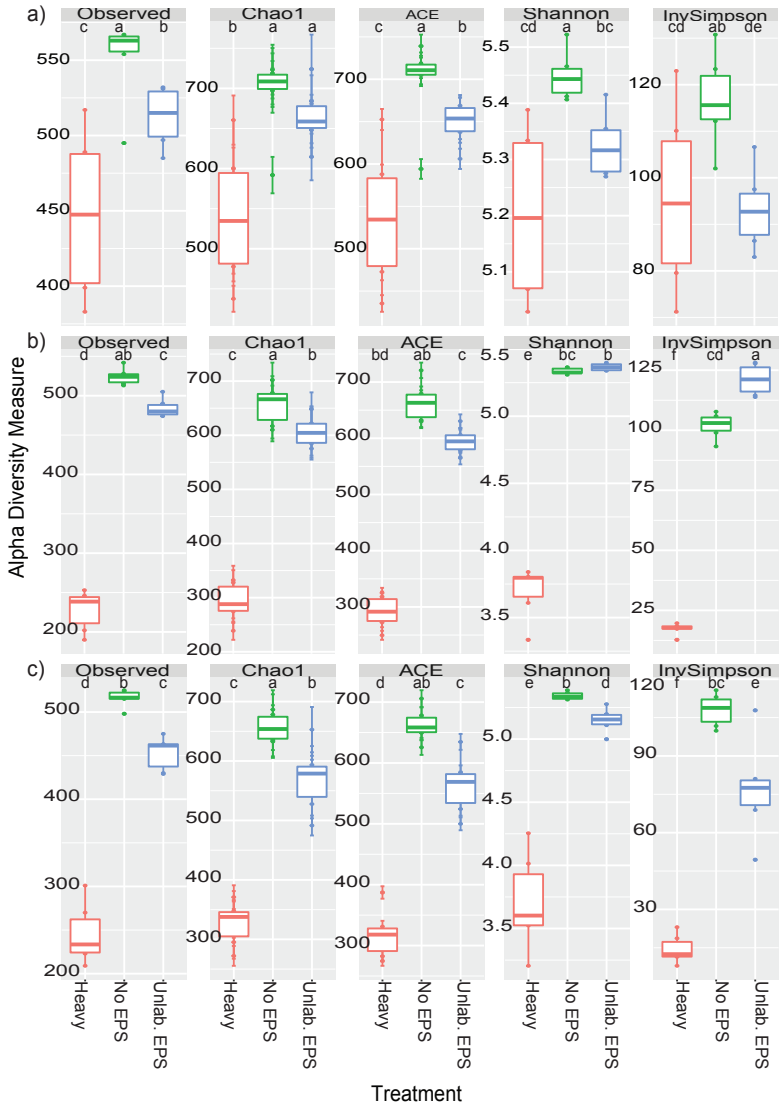

Figure S2: Box-plot comparisons of alpha-diversity assessment by richness estimators (number of observed OTUs, Chao1, ACE) and diversity indices (Shannon, Inverse Simpson) for bacterial 16S rRNA gene samples at different time points. a) day 8; b) day 24; c) day 35. Within each index, identical letters mean no significant difference (p-value < 0.05). Comparisons performed across treatments using ANOVA test and Tukey`s HSD post-hoc test. Data rarefied to the minimum sampling depth. Unlab. EPS-incubation containing ^{12}C-WH15EPS. Heavy – 'heavy fraction' of incubations containing ^{13}C-WH15EPS.

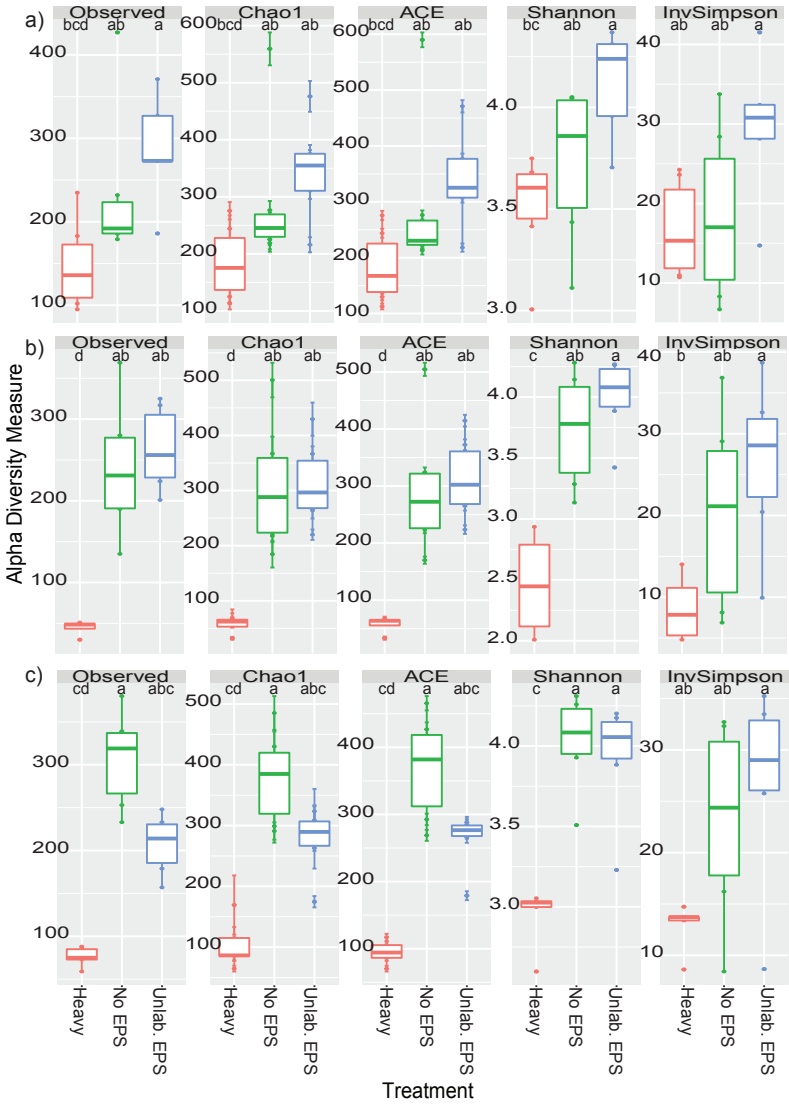

Figure S3: Box-plot comparisons of alpha-diversity assessment by richness estimators (number of observed OTUs, Chao1, ACE) and diversity indices (Shannon, Inverse Simpson) for fungal ITS 1 region gene samples at different time points. a) day 8; b) day 24; c) day 35. Within each index, identical letters mean no significant difference (p-value < 0.05). Comparisons performed across treatments using ANOVA test and Tukey`s HSD post-hoc test. Data rarefied to the minimum sampling depth. Unlab. EPS-incubation containing ^{12}C-WH15EPS. Heavy – 'heavy fraction' of incubations containing ^{13}C-WH15EPS.

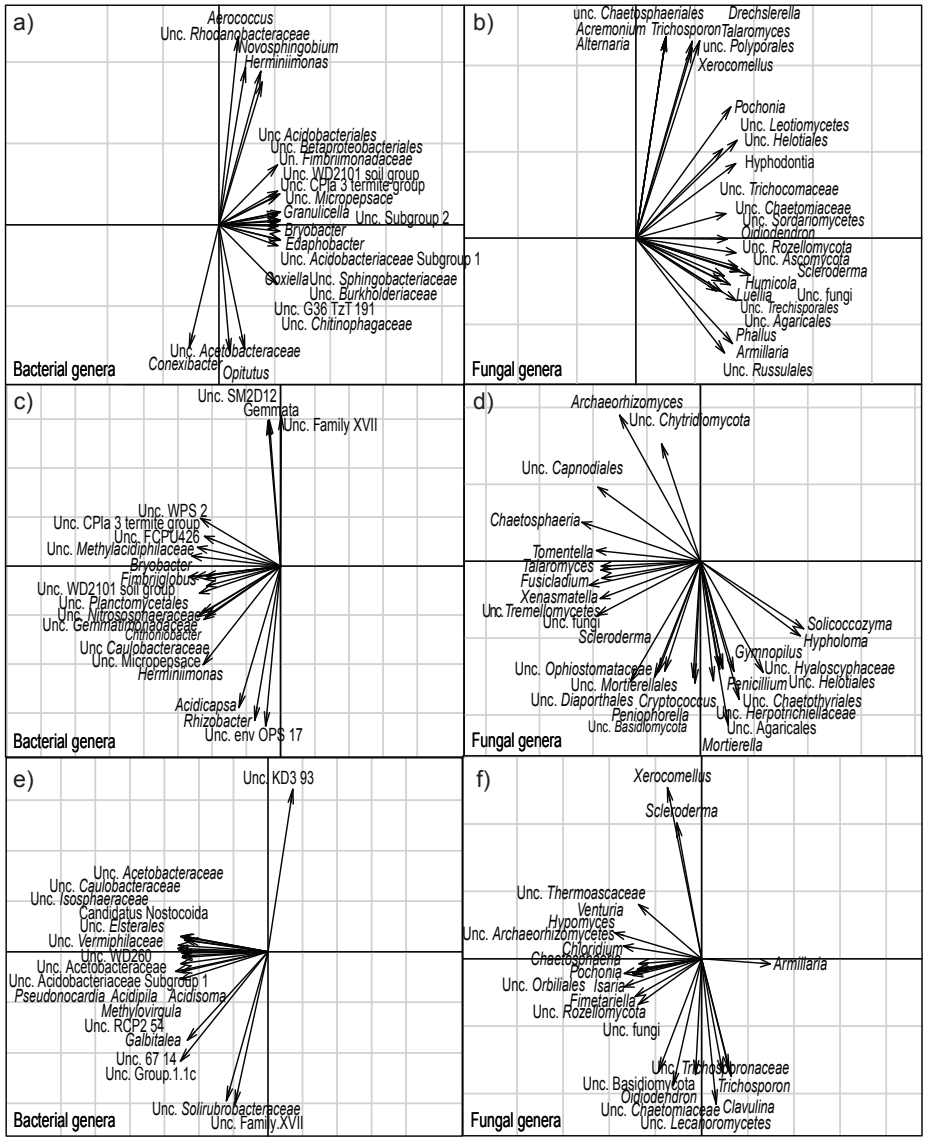

Figure S4: Co-inertia`s (COIA) bacterial and fungal important genera. Top 20 genera of a), c), e) bacteria and b), d), f) fungi that significantly correlated with co-variation of the samples in ^{13}C EPS (a and b), ^{12}C EPS (c and d) and unamended samples (e and f).

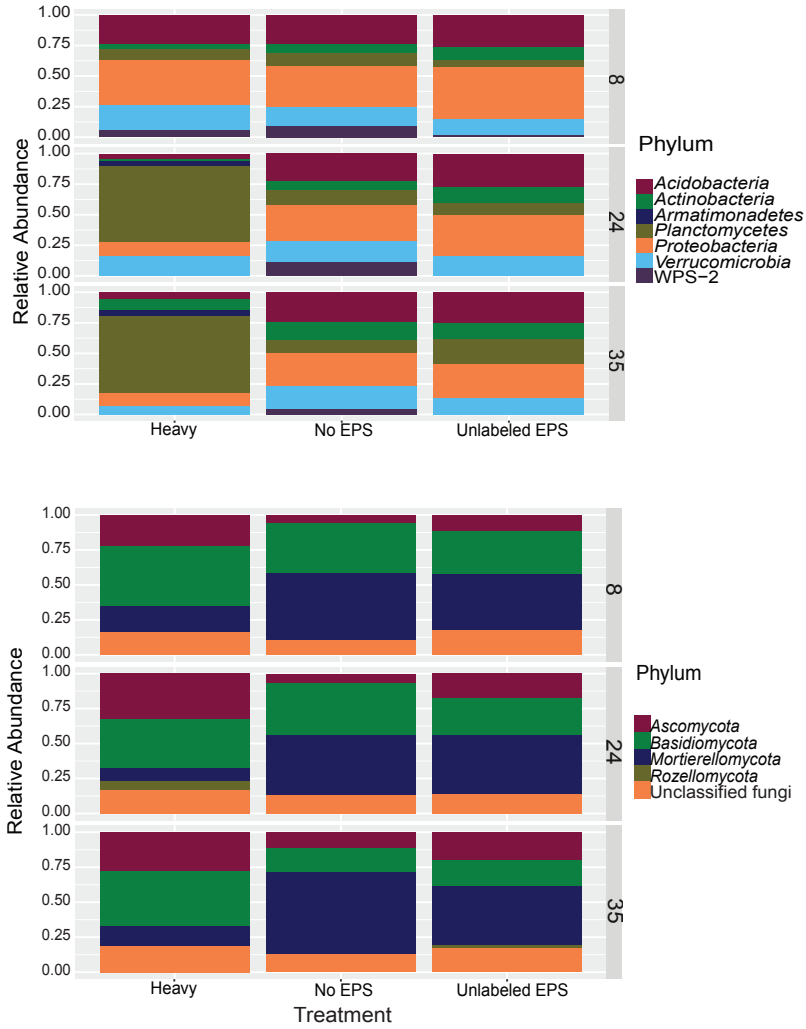

Figure S5: Relative abundance of microbial phyla. Relative abundance of a) bacterial and b) fungal groups at phylum level in heavy fraction, EPS amended (Unlabeled EPS) and unamended (No EPS) controls at all time points (8, 24, 35). Only phyla with >3% abundance are shown.

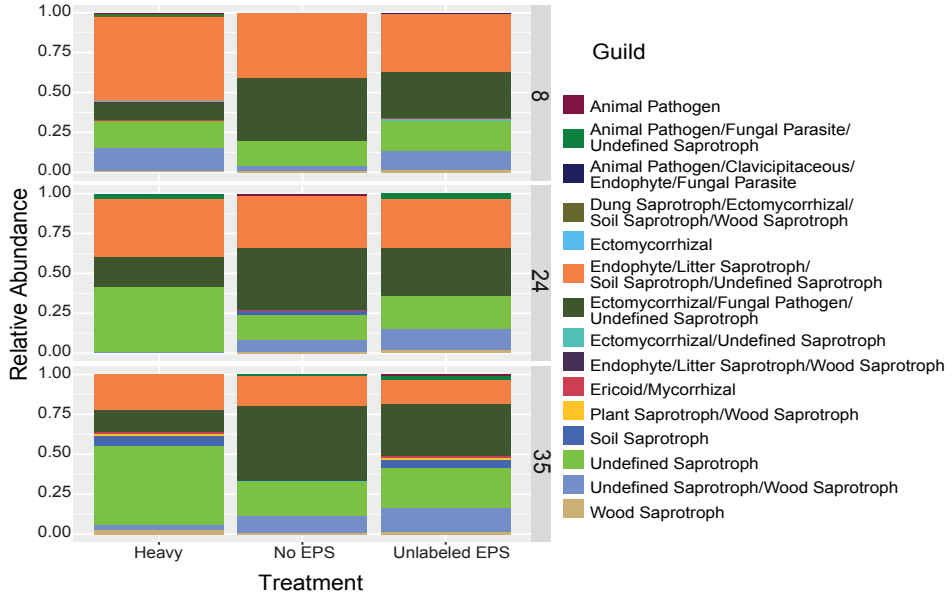

Figure S6: Fungal guilds. Relative abundance of fungal guilds in heavy fraction, EPS amended (Unlabeled EPS) and unamended (No EPS) controls at all time points, based only in the OTUs with assigned guilds (60% of total sequences). Only guilds with >1% abundance are shown.

Table S1: Neighbors of genus *Singulisphaera* and *Granulicella* in co-occurrence network of "heavy" fraction samples.

Group	Phylum	Type of interaction	r-value
Singulisphaera			
Unclassified *Armatimonadales*	*Armatimonadetes*	positive	0.97
Occallatibacter	*Acidobacteria*	positive	0.92
Unclassified Subgroup 2	*Acidobacteria*	negative	-0.81
Conexibacter	*Actinobacteria*	positive	0.90
Unclassified *Solirubrobacterales*	*Actinobacteria*	positive	0.87
Uncultured *Solirubrobacteraceae*	*Actinobacteria*	positive	0.82
Unclassified IMCC26256	*Actinobacteria*	positive	0.82
Uncultured *Acidimicrobiia*	*Actinobacteria*	positive	0.81
Acidothermus	*Actinobacteria*	positive	0.80
Actinospica	*Actinobacteria*	positive	0.75
Unclassified Lineage IV	*Elusimicrobia*	positive	0.82
Uncultured Family XVII	*Firmicutes*	positive	0.86
Candidatus Nostocoida	*Planctomycetes*	positive	0.97
Gemmata	*Planctomycetes*	positive	0.96
Unclassified *Isosphaeraceae*	*Planctomycetes*	positive	0.92
Uncultured *Gemmataceae*	*Planctomycetes*	positive	0.85
Unclassified WD2101 soil group	*Planctomycetes*	negative	-0.82
Uncultured *Pirellulaceae*	*Planctomycetes*	positive	0.97
Anaeromyxobacter	*Proteobacteria*	positive	0.83

Group (continued)	Phylum	Type of interaction	r-value
Unclassified KF JG30 C25	*Proteobacteria*	positive	0.78
Unclassified *Chthoniobacteraceae*	*Verrucomicrobia*	positive	0.93
Uncultured *Methylacidiphilaceae*	*Verrucomicrobia*	positive	0.88
Unclassified *Pedosphaeraceae*	*Verrucomicrobia*	negative	-0.76
Granulicella			
Unclassified *Pedosphaeraceae*	*Verrucomicrobia*	positive	0.88
Unclassified Subgroup 2	*Acidobacteria*	positive	0.85
Edaphobacter	*Acidobacteria*	positive	0.80
Unclassified *Acidobacteriaceae* Subgroup 1	*Acidobacteria*	positive	0.79
Candidatus Koribacter	*Acidobacteria*	positive	0.76
Uncultured_*Acidobacteriales*	*Acidobacteria*	positive	0.75
Acidothermus	*Actinobacteria*	negative	-0.79
Uncultured *Solirubrobacteraceae*	*Actinobacteria*	negative	-0.89
Unclassified 67 14	*Actinobacteria*	negative	-0.82
Uncultured *Acidimicrobiia*	*Actinobacteria*	negative	-0.79
Conexibacter	*Actinobacteria*	negative	-0.75
Mucilaginibacter	*Bacteroidetes*	positive	0.86
Uncultured Family XVII	*Firmicutes*	negative	-0.80
Uncultured *Gemmataceae*	*Planctomycetes*	negative	-0.85
Unclassified WD2101 soil group	*Planctomycetes*	positive	0.76
Uncultured *Xanthobacteraceae*	*Proteobacteria*	positive	0.90
Burkholderia Caballeronia Paraburkholderia	*Proteobacteria*	positive	0.86
Unclassified *WD260*	*Proteobacteria*	positive	0.83
Rhodovastum	*Proteobacteria*	negative	-0.79
Bradyrhizobium	*Proteobacteria*	positive	0.76
Unclassified WPS 2	WPS 2	positive	0.83

Table S2: Neighbors of genus *Singulisphaera* and *Granulicella* in co-occurrence network of unlabeled EPS samples.

Group	Phylum	Type of interaction	r-value
Singulisphaera			
Acidothermus	*Actinobacteria*	positive	0.88
Dyella	*Proteobacteria*	negative	-0.76
Gemmata	*Planctomycetes*	positive	0.76
Rhodanobacter	*Proteobacteria*	negative	-0.76
Unclassified *Armatimonadales*	*Armatimonadetes*	positive	0.79
Unclassified G36 TzT 191	*Proteobacteria*	positive	0.75
Unclassified KF JG30 C25	*Proteobacteria*	positive	0.84
Unclassified *Pedosphaeraceae*	*Verrucomicrobia*	positive	0.83
uncultured *Pirellulaceae*	*Planctomycetes*	positive	0.93
uncultured *Solirubrobacteraceae*	*Actinobacteria*	positive	0.84